

## QUANTITATIVE MAPPING OF HYDRODYNAMIC VEGETATION DENSITY OF FLOODPLAIN FORESTS USING AIRBORNE LASER SCANNING

M.W. Straatsma

Department of Physical Geography, Faculty of Geosciences, Utrecht University, The Netherlands  
PO Box 80115, 3508 TC Utrecht, e-mail: m.straatsma@geo.uu.nl

**KEY WORDS:** airborne laser scanning, floodplains, hydrodynamic vegetation density, forest, simulation

### ABSTRACT:

The determination of hydrodynamic vegetation density of floodplain forests in the Netherlands is currently based on manually delineated vegetation types and a lookup table to convert these into vegetation density. In this paper a method is presented to extract vegetation density from high-density airborne laser scanner data. Field reference data were collected on 45 plots in three different floodplains in the Rhine delta. Two predictors for vegetation density were extracted from the laser data: (1) percentage (P) of points in the height interval inundated by the water, and (2) a vegetation area index (VAI) that corrects for occlusions from the crown area. A computer simulation, using a digital forest model, was carried out to gain more insight in the prediction of vegetation density from laser scanning data. The simulation showed the need for a minimum number of points to accurately compute the predictors and the sensitivity of the predictors for non-returned ground points. P proved the best predictor of vegetation density ( $R^2 = 0.62$ ).

### 1. INTRODUCTION

Safety levels of embanked rivers are computed using hydrodynamic models, which need vegetation roughness as input. For forests, this roughness is determined by the vegetation density ( $D_v$ ), defined by the projected plant area ( $A$ ) in the direction of the water flow ( $F$ ) per unit volume (Petryk & Bosmajian, 1975; Nepf, 1999) (figure 1). Under the assumption of cylindrical vegetation elements, vegetation density can be characterized by the product of number of stems per square meter and stem diameter. Vegetation density is expressed as  $m^2/m^3$ . In the Netherlands an approach is used in which vegetation density values are assigned to floodplain ecotopes. Ecotopes are 'spatial landscape units that are homogeneous as to vegetation structure, succession stage and the main abiotic factors that are relevant to plant growth' (Leuven et al., 2002). In an initial step ecotopes are delineated by manual classification of false color aerial photographs using an interpretation key (Jansen & Backx, 1998). Subsequently, a lookup table converts forest ecotopes to vegetation density (Van Velzen et al., 2003). The disadvantage of this method is the low level of automatisation and the loss of spatial variation of vegetation density within the ecotope mapping units.

Airborne laser scanning enables the automatic extraction of various forest structural characteristics related to vegetation density: stem number, stem diameter, basal area and/or timber volume (Lefsky et al., 1999a; Lefsky et al., 1999b; Means et al., 1999; Næsset, 1997; Næsset & Bjerknes, 2001; Nilsson, 1996; Drake et al., 2002; Holmgren & Jonsson, 2004; Næsset, 2002). Asselman (2002) studied vegetation density of reeds, shrubs and forests. She related vegetation density to the laser-derived 90 percent quantile of the vegetation heights, which showed a fairly strong relation ( $R^2=0.6$ ). However vegetation density has not yet been determined directly based on the inundation height, which is equal to the water depth during flood stage of the river. The objective of this study was to assess the suitability of airborne laser scanning data for the direct quantitative mapping of hydrodynamic vegetation density of lowland floodplains under leaf-off conditions using two methods: (1) relative number of points in the inundation

height, (2) the Vegetation Area Index (VAI) based on the method of MacArthur and Horn (1969). These laser scanning methods were compared to the current ecotope approach.

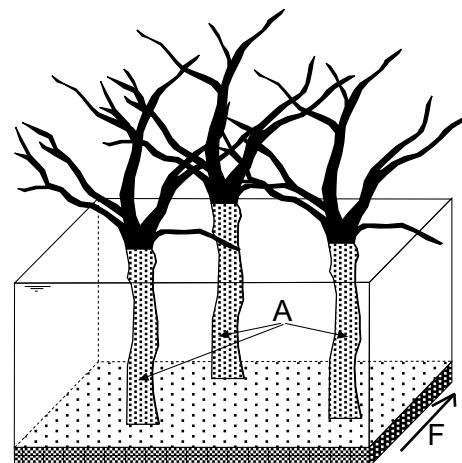


Figure 1: Sketch of hydrodynamic vegetation density ( $D_v$ ); the projected plant area,  $A$ , in the direction of the flow,  $F$  per unit volume

### 2. MATERIALS AND METHODS

#### 2.1 Study area

The study was carried out in three floodplains of the Rhine distributaries in the Netherlands: (1) Duursche Waarden, (2) Afferden en Deestse Waarden and (3) Gumerense Waard. All are characterized by small surface elevation differences. Land cover is a combination of agriculture, meadows, open water and nature areas that partly consisted of forests. Forests comprise softwood forest in various stages of development (willow, (*Salix Alba*, *Salix Viminalis*), poplar (*Populus nigra*, *Populus x canadensis*)), hardwood forest in various stages of development (oak (*Quercus robur*), ash (*Fraxinus excelsior*)) and a small mature pine stand (*Pinus sylvestris*).

## 2.2 Data collection

The following data was available for this study:

- Ecotope map for the whole river area based on visual interpretation of aerial photographs of 1996 (Jansen & Backx, 1998);
- Field measurements (45) of vegetation density in the three floodplains mentioned above. Plots, sized 200 m<sup>2</sup> or more were outlined in the field. Vegetation density was calculated as the product of stem number and stem diameter at breast height. All forests were in winter condition. Field data were collected simultaneously with the laser scanning data;
- FLI-MAP laser data of the same floodplains as mentioned above: small footprint (0.3 m), first pulse, airborne laser scanning data under leaf-off conditions with extremely high point densities (table 1).

Table 1: Metadata for the three laser scanning campaigns

Floodplain <sup>a</sup> location	DW, ADW	GW
Acquisition time	March 2001	March 2003
Scan angle	± 30°	± 30°
Nr of sensors	1	2
Flying height	80 m	80 m
Point density	12	75
Flight strips	Single	Double

<sup>a</sup> DW = Duursche Waarden, ADW = Afferden en Deestse Waarden, GW = Gumerense Waard

## 2.3 Proxies for vegetation density

In the Netherlands, the current method of assigning vegetation density values to floodplain forests and other vegetation types is based on manual delineation of ecotopes from false color aerial photographs and a lookup table (Jansen & Backx, 1998; Van Velzen et al., 2003). To assess the predictive quality of this method linear regression was used with vegetation density based on ecotope maps as independent variable and the observed values of vegetation density in the field as the dependent variable. The predictive quality of the ecotope approach serves as a point for vegetation densities derived from laser scanning.

First step in the laser data processing was the selection of the points located inside the plots delineated in the field. Other laser points were not taken into account. For each plot a Digital Terrain Model (DTM) was constructed using iterative residual analyses based on a simplified version of the method of Kraus and Pfeifer (1998). Heights relative to the DTM were used in subsequent computation.

Vegetation density was predicted from laser scanning data by two methods. The first computes the percentage (P) of laser hits that fall within the height range (h1 to h2) that could be inundated by the water:

$$P_{h1-h2} = \frac{1}{h2 - h1} * \frac{N_{h1-h2}}{N_{tot}} \quad (1)$$

in which N<sub>h1-h2</sub> is the number of points between height 1 and 2 above the forest floor, N<sub>tot</sub> is the total number of points in the field plot including canopy and ground surface points. The height interval for P is 0.5 to 2.5 m, the region around breast height where the vegetation density was measured in the field. Moreover, h1 was not set to zero because ground surface points showed noise, and setting h1 to 0.5 therefore also served to exclude noise. However, this method does not take occlusions from the crown area into account. Tree crowns reflect part of the laser pulses, thereby limiting the number of points available for detection of stems or the ground surface. The second method by MacArthur and Horn (1969) does compensate for occlusions and was verified later by Aber (1979). This method calculates a Leaf Area Index for specific height increments, which is similar to the extinction of light in a semi-transparent medium. Recently, Lefsky et al. (1999b) successfully modified the MacArthur-Horn method to generate canopy height profiles. Canopy height profiles not only include foliage, but also woody vegetation. In the present study all forests were leafless except for the pine stand. Therefore we hypothesize that leafless trees show the same way of occlusion as trees in leaf-on conditions. The resulting value is not a Leaf Area Index, but a Vegetation Area Index (VAI). Like P, the VAI is computed only over the height interval that is inundated by the water using the following equation:

$$VAI_{h1-h2} = \frac{1}{h2 - h1} * \ln\left(\frac{N_{h2}}{N_{h1}}\right) \quad (2)$$

in which N<sub>h1</sub> and N<sub>h2</sub> are the number of points below heights h1 and h2. The first term in the formula is added to make the VAI independent of the height interval. However three assumptions underlie this method: (1) that laser pulses enter parallel into the forests, (2) that the horizontal distribution of vegetation elements is random and (3) that all vegetation elements have an equal angle. Strictly speaking none of these assumptions hold.

## 2.4 Simulation

To gain insight in the effects of not fulfilling the assumptions mentioned in the previous section and the effect of not compensating for occlusions, a computer simulation was carried out for a simplified forest-canopy scheme. The simulation creates a digital forest model and computes the height of intersection between the 'trees' and simulated laser pulses (figure 2).

Trees had a stratified random spatial arrangement and were represented as a rectangular stem shape and a circular horizontal crown. The laser pulses were based on laser scanning settings similar to FLI-MAP; flying height was set to 80 m and the scan angle to ± 30°. By calculating P and VAI for different forest layouts and laser point densities, the following effects were evaluated quantitatively:

- The relation between vegetation density and P and VAI. Using 1 laser point per m<sup>2</sup>, vegetation density was varied stepwise between 0.003 to 0.2 m<sup>2</sup>/m<sup>3</sup>.
- The minimum number of laser points needed in the VAI interval (0.5-2.5 m) for a stable VAI computation. Due to the random effect in the tree distribution, the resulting P and VAI values varied between subsequent model runs. Therefore a suite of simulations was carried out in which point densities were decreased stepwise from 4 points per

$\text{m}^2$  to 1 point per  $400 \text{ m}^2$ . For each point density 30 simulations were run, which enabled the computation of the coefficient of variation as a function of number of points in the VAI and P interval.

- The effect of the number of ground points on the VAI and P value, allowing to determine the effect of loss of returns from the ground surface.
- The effect of the incidence angle on VAI and P. The incidence angle of the laser pulse is not equal over the width of the scan strip. Along the edges the angle is highest leading to a higher probability of hitting a stem due to the longer trajectory through the vegetation and a larger angle between the stem and the laser pulse. For example, at nadir point a laser pulse will never hit a vertical stem. Laser pulses were generated with equal incidence angles over the whole plot. The incidence angle was varied stepwise from 0 to  $40^\circ$  with  $2^\circ$  increments.

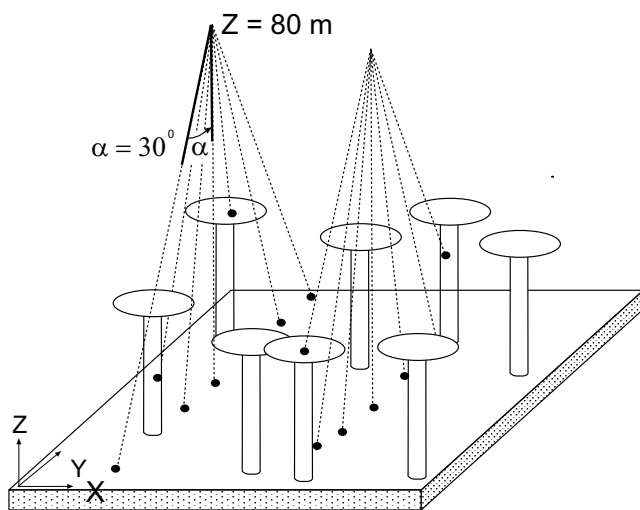


Figure 2: Layout of the simulation

## 2.5 Non-returned ground points reconstruction

Both P and VAI rely on the accurate determination of the number of ground points. The number of ground point influences  $N_{\text{tot}}$  (eq. 1) for P and  $N_{\text{h1}}$  and  $N_{\text{h2}}$  for VAI (eq. 2). However, ground points are sometimes not detected under field conditions, due to; (1) low reflectivity of the ground surface combined with (2) mirroring away at large scan angles or (3) trapping of the reflected pulse in the tree crown. Therefore it

was necessary to reconstruct the original number of emitted pulses over each plot. Average point density of the whole dataset was not sufficient as the plot might be located either in an area of overlapping strips or not. As flight path data was not available, the only information available was the point distribution over the plot area and the challenge was to select the correct point density and multiply that with the surface area of the plot. The following method was used for reconstruction of the total point density. First, vegetation points were omitted from the analyses as extremely high point densities resulted from the three dimensional structure of the trees. Laser hits were classified as vegetation when their height above the DTM was more than 0.4 m. Next, the local point density was computed for each ground point in a circular local window with a 1 m radius, resulting in a distribution of point densities for each plot. A small window size was chosen because in some cases few ground points were present. Increasing the window size would lead to underestimation of the local point density. The 90 percent quantile of the resulting point density distribution was then selected as representative for the whole plot, and was multiplied by the surface area of the plot indicating the total number of expected pulses in the plot. The expected points minus the actually recorded points were assumed to have represented the ground surface, and their number was added to the ground points identified in the laser data for each plot. Finally, P and VAI were computed with the corrected number of ground points.

## 3. RESULTS

### 3.1 Estimates for all field plots

Figure 3 shows the scatter plots between observed vegetation densities in the field and (1) ecotope approach prediction, (2) the percentage (P) of laser points in the inundation height and (3) the Vegetation Area Index. Regression analyses showed that all methods explain little of the variance in vegetation density as measured in the field. The ecotope prediction shows four classes. The vertical range per cluster indicates the range of vegetation densities per ecotope type. P and VAI show a linear relation close to the origin and large outliers, which both underestimate and overestimate vegetation density. Remarkably, the ecotope approach ( $R^2 = 0.30$ ) explains a larger part of the field variation than either P ( $R^2 = 0.08$ ) or VAI ( $R^2 = 0.03$ ).

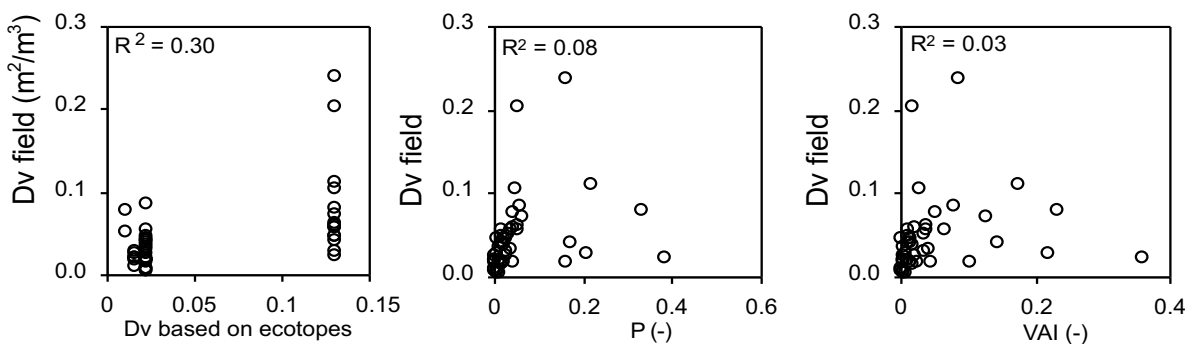


Figure 3: Scatter plots of the ecotopes, P and VAI as predictors of vegetation density for all field plots. All methods (ecotopes, P and VAI) show explain little of the variance of vegetation densities as measured in the field.

### 3.2 Simulation results

Part of the error in predicting the vegetation density might result from not meeting the assumptions of the underlying model used. The simulation results provide insight in the effect of the assumptions. Figure 4a shows that P increases at lower vegetation densities and decreases at higher values. VAI increases linearly with Dv, over the range of vegetation densities from 0.003 to 0.2 m<sup>2</sup>/m<sup>3</sup>. For low vegetation densities, the curves for P and VAI are almost parallel. The horizontal crown and the vertical stem do not inhibit the use of the VAI as a predictor of vegetation density. The influence of the number of points in the height interval ( $N_{h1-h2}$ ) on the determination of VAI is shown in figure 4b. The error bars indicate the standard deviation of the VAI of the 30 simulations. With increasing number of points, the standard deviation and coefficient of variation decrease. A coefficient of variation (CV) of 0.15 was arbitrarily selected as a minimum acceptable level, which is reached when  $N_{h1-h2}$  exceeds 50 points. Furthermore, if the number of ground hits decreases, both P and VAI become higher (figure 4c). This implies that if ground returns remain undetected, VAI and P will be overestimated. VAI is more sensitive to an accurate number of ground returns, particularly at a low number of ground points, indicated by the strong increase of VAI when the number of ground points lower than 20,000. Total number of points was 60,000 in this example. The last assumption underlying the equation is that all laser pulses have the same incidence angle, instead of varying between  $\pm 30^\circ$ . Figure 4d shows the dependence of the P and VAI on incidence angle. At a vegetation density representative for a normal forest ( $Dv = 0.022 \text{ m}^2/\text{m}^3$ ), a stray linear relation was found between incidence angle on one hand and P and VAI on the other over the 0-40° range.

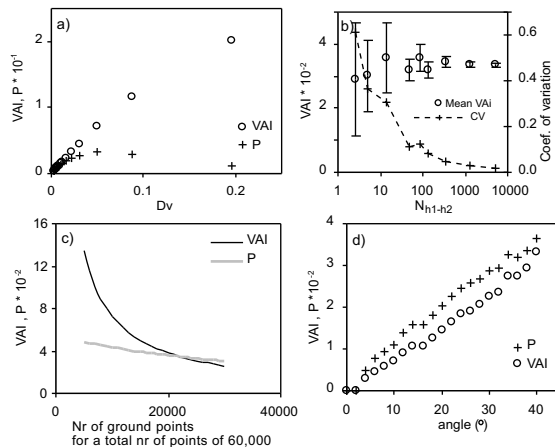


Figure 4: Values obtained for VAI and P from the simulation, which shows the dependance on a) varying Dv, b) number of points in the inundation height, c) Nr of ground points and d) incidence angles.

### 3.3 Estimates for conditioned plots

Based on the simulation results (figure 4b), only those plots that included more than 50 points in the inundation height were considered. Moreover shrub vegetation was excluded due to the very different vegetation structure. Scatter plots of the relation between vegetation density, P and VAI are shown in figure 5 in the upper two panels. Subsequently, the number of lost ground points was reconstructed as described above and P and VAI were recalculated (figure 5 lower panels). Surprisingly P was a better predictor of vegetation density than VAI, both before

and after the correction of the number of lost ground points. Explained variance of P increased from 0.57 to 0.62 when correction for missed ground points were made compared to 0.32 and 0.37 for VAI (table 2). Regression equations did not change due to the ground points correction. No pine forest plots met the minimum required number of points. From this it is concluded that at least 50 laser returns are needed in the height interval of interest and that a correction for lost ground points was important. The resulting relations are valid for deciduous floodplain forest under winter conditions.

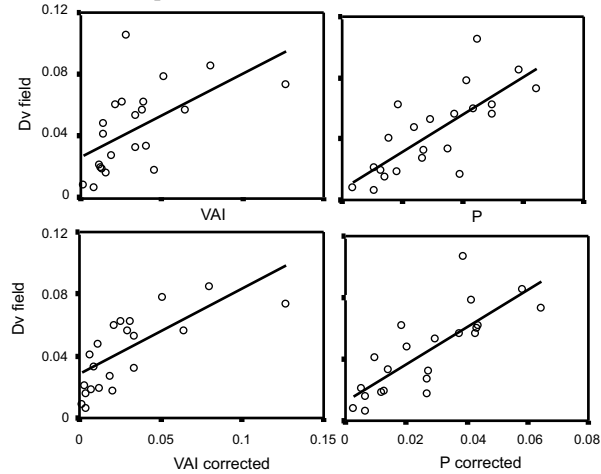


Figure 5: Prediction of vegetation density by P and VAI. The upper two panels are not corrected for missed ground points, lower panels are corrected. Units are the same for each row and column.

Table 2: Regression results for vegetation density prediction

Regression equation	R <sup>2</sup>	RSE <sup>a</sup>
Dv = 1.22*P + 0.01	0.58	0.018
Dv = 1.22*Pcorrected + 0.01	0.62	0.017
Dv = 0.54*VAI + 0.03	0.32	0.023
Dv = 0.55*VAIcorrected + 0.03	0.37	0.022

<sup>a</sup> RSE = Residual standard error

## 4. DISCUSSION

In all plots, straightforward application of equations 1 and 2 to the laser data yielded poor estimates of vegetation density. Explained variance ( $R^2 = 0.08$  to 0.03) was much lower than for the traditional method based on ecotope mapping ( $R^2 = 0.30$ ). The first reason was that the minimum number of points in the inundation height was not reached for many field plots. Therefore the simulation was used to decide upon the minimum number of points needed, which appeared to be 50. Moreover shrub vegetation was excluded due to the different vegetation structure. Exclusion of the plots that did not meet the conditions improved the results significantly. The reason for a low number of laser hits in the inundation height interval can result from a very thick crown layer such as pine forests or from a loss of vegetation hits. The solution for a large amount of occlusion from the crown layer is to increase the plot size to reach the needed number of laser hits. Loss of vegetation hits mostly occurred with young forests. Figure 6 shows a three-dimensional scatter plot of a young oak forest. The number of hits on the vegetation area is much lower than expected based on the vegetation density of 0.11 m<sup>2</sup>/m<sup>3</sup>. The point distribution on the ground surface shows that many points are missing,

these should have been returned from the stems and branches. However, the vegetation apparently did not reflect enough energy to exceed the detection threshold of the laser receiver. Apparently the reflectivity of the bark of this young forest and other young willow shoots is too low to be detected. Waveform digitizing laser scanner might solve this problem, since it does not use a threshold.

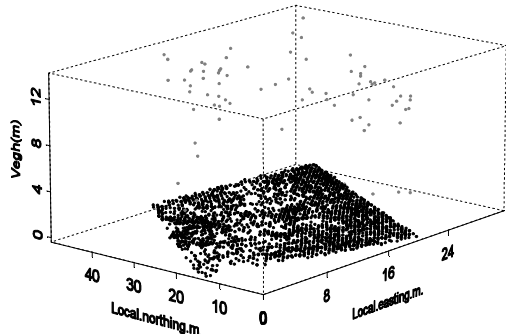


Figure 6: Loss of vegetation hits in young hardwood forests, due to low reflectivity of the bark.

The second reason for the low quality of the initial models (figure 3) was the loss of ground points. Figure 7 shows an example of non-returned ground points in water-filled ditches resulting in a regular pattern of gaps in the data. Compensation for the non-returned ground points improved the predictive quality of both P and VAI. However, for the reconstruction arbitrary choices had to be made on which quantile of the point density distribution was representative for the original point density. This could still lead to an incorrect estimate of the true number of points. Therefore non-returned laser points should be recorded during data acquisition and labelled as missing since this provides the information that something along the path of the pulse absorbed all laser energy.

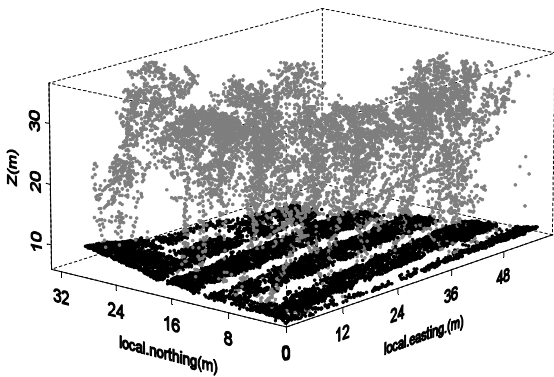


Figure 7: Non-returned ground point in ditches in one of the field plots which is visible as a stripy pattern.

Vegetation density is predicted more accurately by the simple percentage ( $R^2 = 0.62$ ) than by the vegetation area index ( $R^2 = 0.37$ ) (figure 5). This is remarkable because VAI theoretically is a superior model, as it compensates for occlusions by the higher canopy. These models are valid for deciduous forests under leaf-off conditions. The high sensitivity of VAI for accurate determination of the number of ground points is probably the reason for the bad performance of the model. Furthermore, the level of occlusion from the leafless canopy was low, so P was not affected much and the advantage of VAI was limited.

The simulation study showed that a varying incidence angle has a large effect on both P and VAI (figure 4b). The effect on VAI and P of the field plots is potentially large because the size of the field plots was around 20 by 20 meter. Therefore the plots were too small to cover the full width of a scan strip, limiting the range of incidence angles within a single plot, which could lead to large differences of the average incidence angle between plots. Again, reconstruction of the incidence angle afterwards is difficult when the flight path has not been provided, due to gaps in the laser data and an irregular flight path. Therefore, in accordance with the point data record of the ASPRS guidelines (ASPRS, 2003) for laser scanning data, incidence angle should also be exported as an attribute for each point. To improve the detection of vertical stems, scan angles should be increased (figure 4b). Therefore the laser scanner should be rotated to a forward looking direction for floodplain vegetation mapping.

A simulation model is, by nature, a simplification of the real world. In this paper a simple forest-canopy scheme has been used. In a more elaborate ray-tracing model, more effects could be included like a dendritic structure of branches for deciduous trees, leaves, reflectivity of the bark, undergrowth and a threshold for detection of a laser hit, which would increase the insight in the strength of the effect of these parameters. Kay and Kajiyama (1986) show examples of ray tracing of trees, but they used a single light source dissimilar to the moving laser scanner. Adaptation of their model was outside the scope of this paper.

## 5. CONCLUSIONS

This paper described the extraction of hydrodynamic vegetation density from airborne laser scanning data for hydrodynamic modelling. Two different models to predict vegetation density were tested and compared to the traditional ecotope approach: (1) Percentage, which considers the relative number of points in the height interval of interest and (2) the Vegetation Area Index based on the method of MacArthur and Horn (1969). Both predictors have the advantage that they consider a height interval of interest, which in this application is the interval inundated by the water during peak discharges of the river.

Computer simulation of VAI and P based on synthetic data showed that:

- VAI increases linearly with vegetation density while P initially increases and then decreases with increasing vegetation density;
- A minimum number of 50 points per estimate is needed for accurate computation of P and VAI;
- P and VAI strongly increase with higher incidence angles of the laser pulses;
- It is essential to know the total number of emitted points;
- VAI had a stronger dependence on non-returned ground points than P.

P, corrected for missed ground points, is the best predictor ( $R^2 = 0.62$ ) of vegetation density of deciduous floodplain forests under winter condition with little canopy occlusion. This is a large improvement over the ecotope approach ( $R^2 = 0.3$ ). Nevertheless detection of young forests remains problematic because sensitivity of laser receiver was not enough to detect sufficient points on some plots. This might be resolved using full waveform digitizing laser scanning.

To improve vegetation density mapping using airborne laser scanning I recommend to:

- Combine laser scanning data with spectral data to pre-classify the data in pine forest, deciduous forest and shrubs;
- Increase the size of forest field plots for dense canopies to meet the requirement of a minimum number of points in the height interval of interest, and plot size is therefore related to the amount of occlusion;
- Export the incidence angle of the laser pulses during pre-processing of the data to enable correction of the VAI value;
- Record non-returned laser pulses as missing instead of omitting them from the final dataset;
- Change the viewing angle of one of the laser scanners to a more forward direction to detection of vertical stems;
- Investigate in last instance the relation between vegetation density and other parameters such as laser height or standard deviation, which will have to solve the problem of relating tree crown properties to the vegetation density in the inundation height.

#### ACKNOWLEDGEMENTS

This work was funded by NWO, the Netherlands Organization for Scientific Research, within the framework of the LOICZ program. I thank the AGI, the Advisory Board on Geoinformatics and ICT of the Dutch Ministry of Transport, Public Works and Water Management for providing the laser scanner datasets.

#### REFERENCES

- Aber, J.D., 1979. A method for estimating foliage-height profiles in broad leaved forests. *Journal of ecology*, 67, pp. 35-40.
- Asprs, 2003. ASPRS lidar data exchange format standard, URL: <http://www.lasformat.org/~documents/ASPRSformat.pdf>
- Asselman, N.E.M., 2002. Laser altimetry and hydraulic roughness of vegetation, further studies using ground truth. Q3139, WL | Delft Hydraulics, Delft.
- Drake, J.B., Dubayah, R.O., Clark, D.B., Knox, R.G., Blair, J.B., Hofton, M.A., Chazdon, R.L., Weishampel, J.F. and Prince, S., 2002. Estimation of tropical forest structural characteristics using large-footprint lidar. *Remote Sensing of Environment*, 79(2-3), pp. 305-319.
- Holmgren, J. and Jonsson, T., 2004. Large scale airborne laser scanning of forest resources in Sweden. In: M. Thies, B. Koch, H. Specker and H. Weinacker (Editors), *Laser-scanners for forest and landscape assessment*. Institute for forest growth, Freiburg, Germany, Freiburg, Germany.
- Jansen, B.J.M. and Backx, J.J.G.M., 1998. Ecotope mapping Rhine Branches-east 1997, in dutch. 98.054, RIZA, Lelystad.
- Kraus, K. and Pfeifer, N., 1998. Determination of terrain models in wooded areas with airborne laser scanner data. *ISPRS Journal of Photogrammetry and Remote Sensing*, 53(4), pp. 193-203.
- Lefsky, M.A., Cohen, W.B., Acker, S.A., Parker, G.G., Spies, T.A. and Harding, D., 1999a. Lidar Remote Sensing of the Canopy Structure and Biophysical Properties of Douglas-Fir Western Hemlock Forests. *Remote Sensing of Environment*, 70(3), pp. 339-361.
- Lefsky, M.A., Harding, D., Cohen, W.B., Parker, G. and Shugart, H.H., 1999b. Surface Lidar Remote Sensing of Basal Area and Biomass in Deciduous Forests of Eastern Maryland, USA. *Remote Sensing of Environment*, 67(1), pp. 83-98.
- Leuven, R.S.E.W., Gerig, Y., Poudevigne, I., Geerling, G.W., Kooistra, L. and Aarts, B.G.W., 2002. Cumulative impact assessment of ecological rehabilitation and infrastructure facilities in floodplains along the middle reach of the River Waal. In: R.S.E.W. Leuven, I. Poudevigne and R.M. Teeuw (Editors), *Application of Geographic Information systems and remote sensing in river studies*. Backhuys Publishers, Leiden, Backhuys Publishers, pp. 247.
- MacArthur, R.H. and Horn, H.S., 1969. Foliage profile by vertical measurements. *Ecology*, 50(594-598), pp. 1-10.
- Means, J.E., Acker, S.A., Harding, D.J., Blair, J.B., Lefsky, M.A., Cohen, W.B., Harmon, M.E. and McKee, W.A., 1999. Use of Large-Footprint Scanning Airborne Lidar To Estimate Forest Stand Characteristics in the Western Cascades of Oregon. *Remote Sensing of Environment*, 67(3), pp. 298-308.
- Næsset, E., 1997. Estimating timber volume of forest stands using airborne laser scanner data\*1. *Remote Sensing of Environment*, 61(2), pp. 246-253.
- Næsset, E., 2002. Predicting forest stand characteristics with airborne scanning laser using a practical two-stage procedure and field data. *Remote Sensing of Environment*, 80(1), pp. 88-99.
- Næsset, E. and Bjerknes, K.-O., 2001. Estimating tree heights and number of stems in young forest stands using airborne laser scanner data. *Remote Sensing of Environment*, 78(3), pp. 328-340.
- Nepf, H.M., 1999. Drag, turbulence, and diffusion in flow through emergent vegetation. *Water Resources Research*, 35(2), pp. 479-489.
- Nilsson, M., 1996. Estimating tree heights and stand volume using an airborne lidar system. *Remote Sensing of Environment*, 56, pp. 1-7.
- Petryk, S. and Bosmajian, G., 1975. Analysis of flow through vegetation. *Journal of Hydraulics Divisions*, 101, pp. 871-884.
- Ray, T.L., Kajiya, J.T., 1986. Ray tracing complex scenes. *Computer graphics*, 20(4), pp. 269-278.
- Van Velzen, E.H., Jesse, P., Cornelissen, P. and Coops, H., 2003. Flow friction of vegetation in floodplains part 1 (in Dutch). 2003.028, RIZA, Arnhem.